Biomolecules and Biomedicine
ISSN: 2831-0896 (Print) | ISSN: 2831-090X (Online)
Journal Impact Factor® (2025): 2.8
CiteScore® (2025): 4.7
www.biomolbiomed.com | blog.bjbms.org

The BiomolBiomed publishes an "Advanced Online" manuscript format as a free service to authors in order to expedite the dissemination of scientific findings to the research community as soon as possible after acceptance following peer review and corresponding modification (where appropriate). An "Advanced Online" manuscript is published online prior to copyediting, formatting for publication and author proofreading, but is nonetheless fully citable through its Digital Object Identifier (doi®). Nevertheless, this "Advanced Online" version is NOT the final version of the manuscript. When the final version of this paper is published within a definitive issue of the journal with copyediting, full pagination, etc., the new final version will be accessible through the same doi and this "Advanced Online" version of the paper will disappear.

RESEARCH ARTICLE

Blanco et al: Inflammation and lipidomics in HIV

Inflammatory biomarkers and plasma lipidomics after raltegravir plus TDF/FTC initiation in people with HIV: A longitudinal pilot study

Jose-Ramon Blanco[1,2,3], Enrique Bernal-Morell[4,5,6], Santiago Moreno[7,8,9,10], David Rial-Crestelo[10,11,12], María Martínez-Vives[13], Cristina Alonso[13], Leire Pérez-Latorre[10,14,15], Sergio Reus Bañuls[16,17,18], Lourdes Romero[2], Xabier Camino Ortiz de Barrón[19,20], Laura Perez-Martinez[2], CoRIS cohort

[1]Department of Infectious Diseases, Hospital Universitario San Pedro, Logroño, La Rioja, Spain;

[2]Centro de Investigación Biomédica de La Rioja (CIBIR), Fundación Rioja Salud, Logroño, La Rioja, Spain;

[3]Grupo de Investigación en Cuidados y Salud (GRUPAC), Universidad de La Rioja, Logroño, La Rioja, Spain;

[4]Infectious Diseases Section, Department of Internal Medicine, Hospital Universitario Reina Sofía, Murcia, Spain;

[5]Instituto Murciano de Investigación Biosanitaria (IMIB), Murcia, Spain;

[6]Department of Medicine, Universidad de Murcia, Murcia, Spain;

[7]Department of Infectious Diseases, Hospital Universitario Ramón y Cajal, Madrid, Spain;

[8]Instituto Ramón y Cajal de Investigación Sanitaria (IRYCIS), Madrid, Spain;

[9]Department of Medicine and Medical Specialties, Universidad de Alcalá, Alcalá de Henares, Spain;
[10]Infectious Diseases Area (CIBERINFEC), Centro de Investigación Biomédica en Red (CIBER), Madrid, Spain;
[11]HIV Unit, Hospital Universitario 12 de Octubre, Madrid, Spain;
[12]Instituto de Investigación Hospital 12 de Octubre, Madrid, Spain;
[13]Rubió Metabolomics, Derio, Spain;
[14]Department of Clinical Microbiology and Infectious Diseases, Hospital General Universitario Gregorio Marañón, Madrid, Spain;
[15]Instituto de Investigación Sanitaria Gregorio Marañón (IiSGM), Madrid, Spain;
[16]Infectious Diseases Unit, Hospital General Universitario Dr. Balmis, Alicante, Spain;
[17]Instituto de Investigación Sanitaria y Biomédica de Alicante (ISABIAL), Alicante, Spain;
[18]Department of Clinical Medicine, Universidad Miguel Hernández, Sant Joan d'Alacant, Spain;
[19]Department of Infectious Diseases, Hospital Universitario Donostia, Donostia-San Sebastián, Spain;
[20]Instituto de Investigación Sanitaria Biogipuzkoa, Donostia-San Sebastián, Spain.
*Correspondence to **Jose-Ramon Blanco:** jrblancoramos@gmail.com.
DOI: https://doi.org/10.17305/bb.2026.14928

EARLY ACCESS

ABSTRACT

Persistent inflammation and altered lipid metabolism are linked to comorbidities in people with human immunodeficiency virus (HIV), yet their progression after initiating antiretroviral therapy (ART) is not fully understood. This exploratory, uncontrolled pilot study investigated longitudinal changes in biomarkers and plasma lipidomics in 11 ART-naïve adults starting raltegravir plus tenofovir disoproxil fumarate/emtricitabine. Circulating biomarkers were measured, and untargeted plasma lipidomics was performed using ultra-high-performance liquid chromatography–mass spectrometry at baseline and at a follow-up visit near week 48 (range: 47.7–61.9 weeks). Within-participant changes were analyzed using paired Wilcoxon signed-rank tests, with Benjamini–Hochberg false discovery rate (FDR) correction applied separately to biomarker and lipidomic datasets. Paired effect sizes and 95% confidence intervals were also estimated. All participants achieved virological suppression. After FDR correction, interleukin-10 (IL-10) concentrations increased, and soluble cluster of differentiation 163 (sCD163) concentrations decreased (both $q = 0.019$). However, none of the 490 lipid features remained significant after FDR correction. Twenty-six features showed large absolute paired Hedges' effect-size estimates ($|g_z| \geq 0.80$), with 24 positive and two negative estimates. These findings demonstrate longitudinal changes in IL-10 and sCD163 following ART initiation. The lipidomic results, however, are considered hypothesis-generating. Due to the absence of a comparator group, these changes cannot be definitively attributed to the specific ART regimen. Larger, controlled studies are necessary to confirm reproducibility and clinical relevance.

Keywords: HIV, inflammatory markers, lipidomics, raltegravir.

EARLY ACCESS

INTRODUCTION

Antiretroviral therapy (ART) has transformed HIV infection into a chronic, manageable disease with near-normal life expectancy. Nonetheless, persistent immune activation and systemic inflammation remain hallmarks of treated HIV and are strong predictors of non-AIDS comorbidities and adverse clinical outcomes [1]. Which biomarkers best capture these processes remains unresolved, and the extent to which distinct ART regimens differentially modulate inflammatory and metabolic pathways is incompletely defined.

Although integrase strand transfer inhibitor (INSTI)-based regimens have demonstrated more favorable effects on lipid parameters and cardiovascular biomarkers compared with protease inhibitor (PI)-based therapies [2], accumulating evidence links INSTIs to adverse metabolic outcomes [3, 4].

Lipids are central regulators of cellular signaling, membrane dynamics and barrier integrity, and lipid dysregulation is linked to cardiometabolic, hepatic, and neurodegenerative diseases that are disproportionately prevalent in people living with HIV (PLWH) [5]. Beyond total lipid levels, fatty acid composition is a critical determinant of risk: saturated fatty acids are associated with diabetes, whereas polyunsaturated fatty acids are associated with reduced cardiovascular risk and mortality [6]. At the mechanistic level, saturated fatty acids activate myeloid inflammatory pathways, whereas polyunsaturated fatty acids suppress inflammasome signaling and lipopolysaccharide-driven endothelial activation [7].

Initiation of ART induces substantial remodeling of the plasma lipidome in ART-naïve PLWH, and species-resolved changes across lipid classes may provide mechanistically informative biomarkers of ART-related dyslipidemia and cardiometabolic risk beyond conventional lipid measures [8]. In a randomized study of ART-naïve individuals receiving tenofovir/emtricitabine (TDF/FTC) plus efavirenz, ritonavir-boosted atazanavir, or zidovudine/abacavir, longitudinal lipidomic profiling revealed marked and regimen-dependent remodeling, with differences in 72 lipid species spanning seven lipid classes by week 48 [8]. Several of the lipid species and classes most strongly altered following ART initiation have previously been linked to subsequent cardiovascular events in PLWH, supporting the use of lipidomics to

EARLY ACCESS

examine the relationships among ART exposure, viral suppression, and cardiometabolic risk.

More broadly, lipidomics has emerged as a powerful approach to elucidate disease mechanisms, identify clinically relevant biomarkers, and inform therapeutic strategies [9]. Lipids are not merely structural components of membranes but also active regulators of cellular signaling, membrane trafficking, apoptosis, and immune cell function, with biological effects that are highly specific to individual lipid species [10]. Disruption of lipid homeostasis contributes to cardiovascular disease (CVD), infections, and cancer [11]. In HIV, altered lipidomic profiles may function both as markers and mediators of chronic inflammation and ART-associated metabolic stress [12, 13]. Despite this potential, comprehensive lipidomic profiling in PLWH remains limited.

INSTIs are now preferred components of first-line ART globally owing to their potent virological suppression, favorable tolerability, and overall safety profile [14]. Second-generation INSTIs, such as dolutegravir and bictegravir, are prioritized in current treatment guidelines; however, raltegravir (RAL) retains clinical relevance in selected populations, particularly in the context of polypharmacy, renal impairment, or intolerance to newer agents. RAL combined with TDF/FTC has demonstrated robust efficacy in ART-naïve individuals, minimal drug–drug interactions, and a low burden of neuropsychiatric or metabolic adverse effects [14].

Although ART is generally safe and effective, treatment initiation can precipitate metabolic perturbations, including dyslipidemia, impaired glucose tolerance, and changes in body composition. Although INSTIs are associated with potent viral suppression and are generally well tolerated [15], the biomarker and lipidomic changes following initiation of RAL/TDF/FTC remain insufficiently characterized. Prior studies have largely relied on cross-sectional designs, isolated biomarkers, or targeted lipid panels, limiting insight into coordinated immunometabolic remodeling following ART initiation.

To address this gap, we performed a longitudinal study in ART-naïve individuals initiating RAL/TDF/FTC, integrating inflammatory, immune-activation, endothelial, adipokine, and tryptophan-catabolism biomarkers with comprehensive untargeted lipidomic profiling. This systems-level approach was designed to characterize

EARLY ACCESS

coordinated immune–metabolic changes and exploratory lipidomic changes that may not be apparent when individual biomarkers or restricted lipid classes are examined in isolation.

This exploratory pilot study was designed to characterize within-participant changes in circulating biomarkers and lipid features and to generate hypotheses for future research. It was not designed to attribute the observed changes specifically to RAL plus TDF/FTC.

MATERIALS AND METHODS

Ethics statement

Initial approval for this study was granted by the Comité Ético de Investigación de La Rioja (CEImLAR), which served as the reference ethics committee (Ref. CEImLAR EOm 113). Approval was subsequently obtained from the ethics committees of all participating institutions. All participants provided written informed consent for the collection and storage of blood samples and associated personal and clinical data. The CoRIS cohort was approved by the Research Ethics Committee of Hospital General Universitario Gregorio Marañón. All procedures were conducted in accordance with applicable guidelines and regulations, including the Declaration of Helsinki.

Participants

In this study, we included ART-naïve adults (aged ≥18 years) with confirmed HIV-1 infection. All participants initiated RAL plus TDF/FTC, as prescribed by their treating physician during routine clinical care and remained on this regimen until follow-up sample collection. Follow-up samples were collected 47.7-61.9 weeks after treatment initiation.

Eligible participants were required to have a baseline CD4+ T-cell count of at least 200 cells/μL. Exclusion criteria included hepatitis B or C coinfections, new AIDS-defining conditions within 30 days of screening, pregnancy, established CVD, or diabetes mellitus.

EARLY ACCESS

The participants, biological samples, inflammatory biomarker measurements, lipidomic data, and analyses included in the present study have not been reported in, or shared with, any previous publication from our research group.

Blood samples

Data were obtained from the Spanish HIV-positive cohort (CoRIS), and biological samples collected at baseline and approximately 48 weeks after regimen initiation were provided by the HIV BioBank integrated within the Spanish AIDS Research Network. Briefly, CoRIS is a multicenter cohort that collects a standardized dataset, including sociodemographic, immunological, and clinical information at baseline and during follow-up [16, 17]. This cohort is linked to a centralized biorepository, the Spanish HIV Hospital Universitario Gregorio Marañón Biobank (HIV HUGM BioBank) [18]. Participating centers follow standardized protocols to collect an initial blood sample before ART initiation and, when possible, additional samples annually during follow-up. All participants provided informed consent for the storage and use of their biological samples in the biobank. To ensure confidentiality and compliance with ethical standards, the authors had no access to personally identifiable information from the participants.

The analytic sample comprised 11 participants identified within the CoRIS BioBank according to the predefined inclusion and exclusion criteria and the availability of paired baseline and follow-up samples. Therefore, these participants did not represent consecutive eligible cases.

Baseline samples were collected before ART initiation. Because this was an observational cohort study, follow-up sampling was not performed at a fixed protocol-defined time point. Therefore, for each participant, the available follow-up sample collected closest to week 48 (W48) was selected; collection times ranged from 334 to 433 days (47.7-61.9 weeks) after treatment initiation.

Samples were collected and processed according to the standard operating procedures of the CoRIS BioBank. However, because archived biobank samples were used, fasting status could not be confirmed for all participants. Information on BMI, lipid-lowering therapy, conventional lipid profiles, smoking, alcohol consumption and concomitant medications was not consistently available for all participants and was

EARLY ACCESS

therefore not included in the analysis. To limit major metabolic confounding, individuals with diabetes mellitus or established cardiovascular disease were excluded according to the predefined eligibility criteria.

Circulating biomarkers

We assessed a panel of circulating biomarkers, grouped into six categories: (a) pro-inflammatory markers: C-reactive protein (CRP), tumor necrosis factor (TNF), interleukin (IL)-6, and IL-8; (b) the anti-inflammatory cytokine IL-10; (c) immune activation markers: CD40, soluble CD14 (sCD14), soluble CD163 (sCD163), and lipopolysaccharide-binding protein (LBP); (d) endothelial and vascular dysfunction markers: intercellular adhesion molecule-1 (ICAM-1), vascular cell adhesion molecule-1 (VCAM-1), endothelial selection (E-selectin), platelet selectin (P-selectin); soluble P-selectin (sP-selectin) (e) metabolic and adipokine markers: leptin and adiponectin; and (f) tryptophan catabolism markers: tryptophan, kynurenic acid, and quinolinic acid.

The KQ ratio was calculated as kynurenic acid divided by quinolinic acid. Because both metabolites were measured in the same units, the resulting ratio was dimensionless.

sCD14, CD40, LBP, TNF, sCD163, ICAM-1, IL-6, IL-8, IL-10, E-selectin, P-selectin, VCAM-1, and adiponectin were quantified using human magnetic Luminex Discovery assays (Bio-Techne, Minneapolis, MN, USA; catalog no. LXSAHM), following the manufacturer´s instructions. CRP, leptin, sP-selectin, tryptophan, kynurenic acid, and quinolinic acid were quantified using enzyme-linked immunosorbent assay (ELISA) kits according to the manufacturer´s instructions.

This exploratory study was not designed to estimate study-specific within-batch or between-batch coefficients of variation (CVs); therefore, formal intra- and inter-batch CVs were not calculated. Representative intra- and inter-assay imprecision metrics were provided by the manufacturers for the ELISA kits in the corresponding datasheets. For the Luminex Discovery assays used here, the supplier indicates that assay performance is laboratory- and operator-dependent and does not provide assay-specific CV estimates for each implementation; however, the manufacturer indicates

EARLY ACCESS

expected values of <20% intra-assay CV and <30% inter-assay CV. These values reflect manufacturer performance expectations rather than empirical estimates derived from this dataset.

Metabolite extraction and liquid chromatography–mass spectrometry (LC-MS) analysis

LC-MS-grade solvents were obtained from Sigma-Aldrich (St. Louis, MO, USA) and Fisher Scientific (Pittsburgh, PA, USA). Metabolite standards were purchased from Sigma-Aldrich, Avanti Polar Lipids (Alabaster, AL, USA), and Larodan Fine Chemicals (Malmö, Sweden). Plasma samples were fractionated according to their physicochemical properties using solvent-based extraction methods, as described by Barr et al. [19].

For (i) Platform 1 (fatty acyls, bile acids, steroids, and lysoglycerophospholipids), proteins were precipitated with methanol (4:1, v/v) spiked with non-endogenous standards. After vortexing and incubation at -20 °C for 1 h, samples were centrifuged (18,000 × g, 15 min). Aliquots (10 µL) were used for amino acid profiling; the remainder was dried, reconstituted in methanol, and analyzed by UHPLC-MS.

For (ii) Platform 2 (glycerolipids, cholesteryl esters, sphingolipids, and glycerophospholipids), plasma was mixed with NaCl (50 mM) and $CHCl_3$:MeOH (2:1, v/v), vortexed, incubated at -20 °C for 1 h, and centrifuged (16,000 × g, 15 min). The organic phase was dried, reconstituted in acetonitrile:isopropanol (1:1), centrifuged (18,000 × g, 5 min), and analyzed by UHPLC-MS.

Quality control (QC) samples included calibration and validation reference serum/plasma for analytical monitoring and preprocessing validation, as well as QC blanks and system-suitability blanks for background and solvent control. Samples were injected in randomized order, with QC samples interspersed throughout the analytical batches.

LC-MS instrumentation

Ultra-high-performance liquid chromatography (UHPLC) was performed using ACQUITY UPLC systems (Waters Corp., Milford, MA, USA). Mass spectrometric

EARLY ACCESS

detection was performed using an LCT Premier XE ToF system for platform 1 and a Xevo G2 QToF system for platform 2 (both from Waters Corp.). Analytical performance was monitored using repeated injections of QC samples. Retention time variability was <6 s, and mass errors were <5 ppm (m/z 400–1000) and <1.2 mDa (m/z 50–400).

Lipid classification

All entities were assigned to the following LIPID MAPS (Lipid Metabolites and Pathways Strategy) superclasses [20]: fatty acyls (FA), glycerolipids (GL), glycerophospholipids (GP), sphingolipids (SP), and sterol lipids (ST). The corresponding subclasses included: acylcarnitines (CAR); bile acids (BA; free; glycine-conjugated, Gly-BA; taurine-conjugated, Tau-BA); steroids; mono/di/triacylglycerols (MAG/DAG/TAG); phosphatidylcholines, phosphatidylethanolamines, and phosphatidylinositols (PC/PE/PI; diacyl and ether/plasmalogen forms); lysophosphatidylcholines, lysophosphatidylethanolamines, and lysophosphatidylinositols (LPC/LPE/LPI); ceramides (Cer); monohexosylceramides (HexCer); sphingomyelins (SM); and cholesteryl esters (CE).

Quality control

Data generated by UHPLC-ToF-MS were preprocessed using the TargetLynx application manager for MassLynx (Waters Corp.). The initial LC-MS feature table comprised 509 analytical features, each defined by a retention-time and mass-to-charge ratio pair (RT–m/z). Features were annotated before statistical analysis. Approximately 15% were confirmed using authentic reference standards, requiring concordance in accurate mass, retention time, and MS/MS fragmentation. For features with m/z values of 400-1000 Da, confirmation required a retention-time deviation of <3 s and a mass error of <3 ppm. For features with m/z values <400 Da, the same retention-time criterion and a mass

tolerance of 1.2 mDa were applied. Features without authentic standards were putatively annotated using accurate-mass MS/MS fragmentation data acquired in positive and negative electrospray ionization modes and matched against curated lipid databases, in accordance with established lipidomics identification practices [19].

EARLY ACCESS

Raw chromatographic peak areas were normalized according to the procedure described by Martínez-Arranz et al. [21]. No additional statistical batch-correction algorithm was applied. Samples were injected in randomized order, with calibration and validation QC samples interspersed throughout the analytical sequence. Platform 1 was analyzed across four batches and platform 2 across two batches. Analytical reproducibility was assessed separately for each platform using within-batch and between-batch coefficients of variation. The mean inter-batch CVs for the calibration and validation QC samples were 5.34% and 8.41%, respectively, for platform 1, and 3.92% and 8.81%, respectively, for platform 2.

Features were excluded from quantitative analysis when >30% of measurements fell outside the assay's validated linear dynamic range. Eighteen analytical features, corresponding to 15 metabolite identities, failed this criterion: cholesteryl esters CE(18:1), CE(18:2), CE(20:3), CE(20:4), CE(20:5), and CE(22:6); phosphatidylcholine PC(34:2); lysophosphatidylcholines PC(14:0/0:0), PC(16:0/0:0), PC(18:0/0:0), PC(18:1/0:0), and PC(18:2/0:0); dehydroepiandrosterone sulfate; and triacylglycerols TG(52:2) and TG(52:3). The difference between 15 identities and 18 excluded features reflects multiple chromatographically resolved isomeric features, which were treated as independent variables in the LC-MS dataset. After data curation, 490 analytical features, including isomeric features, were retained for analysis.

Sample-size considerations

This study was designed as an exploratory pilot analysis using the available paired baseline and week-48 samples from participants receiving a uniform RAL plus TDF/FTC regimen. No formal a priori power calculation was performed. Given the limited sample size, the analyses were considered hypothesis-generating and estimation-focused, with emphasis on paired effect-size estimates and 95% confidence intervals rather than confirmatory hypothesis testing.

Statistical analysis

For statistical analyses, follow-up was defined as the available time point closest to 48 weeks after ART initiation for each participant (range, 47.7–61.9 weeks). Baseline characteristics were summarized as medians and interquartile ranges (IQRs) for continuous variables and as frequencies and percentages for categorical variables.

EARLY ACCESS

Given the exploratory pilot design, small sample size (n = 11), and the absence of an assumption of normality for the analyte distributions, longitudinal changes from baseline to follow-up were assessed using two-sided paired Wilcoxon signed-rank tests. Analyses were based on observed complete pairs. Baseline and follow-up concentrations are reported as median (Q1-Q3).

For each paired comparison, the within-participant difference was defined as the follow-up value minus the baseline value. Exact Wilcoxon signed-rank inference was used when supported by the observed difference structure and the software implementation; otherwise, the normal approximation was used. The method applied to each analysis is reported in the Supplementary Material. Paired changes were summarized using the Hodges-Lehmann (HL) pseudomedian shift estimate and its 95% confidence interval (CI).

To complement rank-based inference, paired Hedges' g_z was calculated as the mean within-participant change from baseline to follow-up divided by the standard deviation of these changes, with a small-sample bias correction. The correction factor was J = 1 - 3/[4(n-1)-1], where n was the number of complete pairs, and $g_z = Jd_z$ [22]. Ninety-five percent CIs were estimated using 10,000 bootstrap resamples. Positive values indicated increases and negative values indicated decreases from baseline to follow-up. The threshold $g_z \geq 0.80$ was used descriptively and did not define statistical significance.

To account for multiple testing, p values were adjusted using the Benjamini-Hochberg false discovery rate (BH-FDR) procedure. The direct biomarker panel and the lipidomic dataset were treated as separate prespecified multiplicity families, and statistical evidence after multiplicity correction was defined as $q < 0.05$. The KQ ratio and CD4 cell count were analyzed separately as prespecified derived and clinical immunological outcomes, respectively, and were not included in their respective primary FDR families. Sensitivity analyses were additionally performed by incorporating KQ into the biomarker family, incorporating both KQ and CD4 into a broader clinical family, and applying a global BH-FDR correction across all analyzed outcomes.

Because the study comprised a single longitudinal cohort, the primary lipidomic analyses were restricted to within-participant baseline-to-follow-up comparisons; no

EARLY ACCESS

between-group analyses were performed. BH-FDR correction was applied across the lipidomic feature family independently of the biomarker family.

Missing values in educational attainment and HIV transmission route were imputed using multiple imputation by chained equations (MICE). Five imputed datasets were generated with 20 iterations. Educational attainment was imputed using logistic regression, whereas HIV transmission route was imputed by random sampling from the observed categories because logistic regression produced perfect-separation warnings. CD4 cell count, viral load, age, sex, and country were included as predictors but were not imputed. Two missing lipidomic values, one for 18:1n-x_02 and one for 17:0, were imputed within the same MICE framework. All other lipidomic variables and longitudinal outcomes were analyzed using observed complete pairs.

Exploratory Spearman rank correlations were calculated between lipid features showing large observed paired effects $g_z \geq 0.80$ and the prespecified biomarkers IL-10, sCD163, IL-8, and sP-selectin, separately at baseline and follow-up. Spearman correlation coefficients (rho) were reported with bootstrap 95% CIs, nominal p values, and descriptive BH-FDR-adjusted q values. Given the small sample size and post hoc feature selection, these analyses were considered descriptive and hypothesis-generating and were not used to support confirmatory biological or mechanistic conclusions.

All statistical tests were two-sided. An FDR-adjusted $q < 0.05$ was considered evidence of statistical significance for analyses subject to multiplicity correction. Given the exploratory nature of this pilot study, interpretation emphasized paired change estimates, effect sizes, their 95% CIs, and FDR-adjusted results rather than nominal p values in isolation.

Statistical analyses were performed in R (R Core Team, 2011; http://cran.r-project.org).

RESULTS

Eleven ART-naïve PLWH were included in the study (median age, 36.5 years; IQR, 31.3-45.3); 72.7% were male. Most participants were born in Spain (54.5%), had not

EARLY ACCESS

completed a university education (72.7%), and reported sexual transmission (72.7%). At baseline, the median CD4+ T-cell count was 439 cells/μL (IQR, 311-676) and the median plasma HIV-1 RNA level was 86,100 copies/mL (IQR, 5,719-138,666). At the follow-up assessment, the median CD4+ T-cell count increased to 724 cells/μL (IQR, 637-936; unadjusted p = 0.004), and all participants achieved virological suppression.

At follow-up, two circulating biomarkers met the prespecified BH- FDR correction. IL-10 concentrations increased from baseline to follow-up (HL change, ΔHL = 20.675; 95% CI, 15.268 to 43.726; $p < 0.001$; q = 0.019), whereas concentrations of the monocyte/macrophage activation marker sCD163 decreased (ΔHL = -357.966; 95% CI, -818.026 to -173.161; p = 0.002; q = 0.019). No other biomarker remained significant after FDR correction (**Table 1**).

Individual paired trajectories were consistent with these longitudinal changes, showing an overall increase in IL-10 and a decrease in sCD163 between baseline and follow-up (**Figure 1**). In contrast, IL-8 and P-selectin did not meet the FDR-adjusted significance threshold, although both had positive longitudinal effect estimates.

The KQ ratio, analyzed separately as a derived metabolic endpoint, had a median (IQR) of 3.08 (2.58-3.78) at baseline and 3.07 (2.96-3.43) at follow-up (p = 1.00).

Among the 490 lipid features included in the final analysis, 55 (11.2%) had unadjusted p values < 0.05; however, none remained statistically significant after BH-FDR correction.

Twenty-six lipid features had large observed absolute effect-size estimates Hedges' $g_z \geq 0.80$, comprising 24 positive and two negative changes from baseline to follow-up. Given the small sample size and the absence of FDR-significant findings, these effect-size estimates are presented strictly as exploratory and hypothesis-generating. Complete results for all lipid features, including paired change estimates, p values, FDR-adjusted q values, and effect sizes with 95% CIs, are provided in **Supplementary Table 1**, whereas the 26 features meeting the exploratory Hedges' $g_z \geq 0.80$ threshold are summarized in **Supplementary Table 2**. The overall distribution of lipidomic effect-size estimates by lipid class is shown in **Supplementary Figure 1**. The 26 features meeting the exploratory Hedges' $g_z \geq 0.80$ threshold are summarized

EARLY ACCESS

in **Supplementary Table 3**, together with their metabolic class, annotated biological role, and HMDB identifier, where available.

Lipid-biomarker correlations. Exploratory Spearman correlation analyses between selected lipid features and inflammatory biomarkers revealed no significant associations (data not shown). Given the limited sample size, these analyses were considered purely descriptive and exploratory, and were not used to support biological or mechanistic conclusions.

DISCUSSION

The principal contribution of this study is the longitudinal characterization of lipidomic profiles from baseline to follow-up after initiation of INSTI-based therapy, together with their integrated analysis in relation to inflammatory biomarkers. In this longitudinal pilot study of 11 ART-naïve PLWH initiating RAL/TDF/FTC, IL-10 increased and sCD163 decreased after correction for multiple testing. In contrast, none of the 490 lipid features remained significant after FDR correction, although 26 had large absolute observed standardized effect-size estimates. These lipidomic findings should therefore be considered exploratory and cannot establish effects specific to RAL/TDF/FTC in the absence of a comparator group.

All findings should be interpreted within the exploratory nature of this pilot study. The small sample size results in considerable uncertainty around effect-size and correlation estimates, and apparently large effects may represent sampling extremes. Consequently, lipid-specific and correlation findings require replication in larger independent cohorts.

Host lipid metabolism is recognized as an integral component of HIV-associated immune dysregulation. Distinct lipid classes have been associated with inflammatory and immune-activation markers across disease stages and during ART, linking lipidomic remodeling with clinical outcomes [11, 23]. Bowman et al. [23] reported that ART-treated PLWH had a saturated fatty acid-enriched lipidomic profile, dominated by palmitate (16:0) and stearate (18:0), that correlated positively with monocyte activation (CD40, HLA-DR, TLR4, and sCD36) and systemic inflammation (LBP, CRP), whereas polyunsaturated fatty acids showed inverse

EARLY ACCESS

associations with immune activation. These findings support lipid species-resolved measures as potential correlates of HIV-associated inflammation.

In a prospective cohort free of CVD and carotid plaque at baseline, twelve lipid species spanning ten lipid classes were associated with incident carotid plaque-Most of these species were elevated in PLWH, particularly among those receiving ART [5]. These observations suggest an association among HIV, ART exposure, lipidomic alterations, and atherosclerotic risk but do not establish causality.

A lipidomics ancillary analysis of the ACTG A5257 randomized trial identified ART class–specific lipidome remodeling, with PI-based regimens (ATV/r or DRV/r) inducing significantly larger shifts in glycerophospholipids and sphingolipids than the INSTI-based regimen (RAL). Several species showed changes in opposite directions under RAL versus PI therapy, including lysophosphatidylcholine (LPC(16:1), LPC(17:1), LPC(20:3)) and phosphatidylcholine (PC(40:7), PC(38:4)), with additional divergence observed for ceramides, phosphatidylcholines, phosphatidylethanolamines, and sphingomyelin [13]. Overall, lipidomic perturbations were smaller with RAL than with boosted PI regimens in that trial.

Although our results can be considered alongside those of ACTG A5257 [13], the absence of a comparator group and of FDR-significant lipid changes prevents us from concluding that RAL produced an attenuated or lipid-neutral profile relative to other ART regimens.

In a metabolically controlled longitudinal SIV model, phosphatidylethanolamines (PE), lysophosphatidylethanolamines (LPE), and phosphatidylcholines (PC) were largely unchanged by SIV infection itself but exhibited significant and sustained reductions during ART [11]. Although these findings indicate treatment-associated remodeling in that model, their applicability to the present human cohort remains uncertain.

Despite effective ART, PLWH remain at elevated cardiovascular risk, in part because immune activation and inflammation can persist despite viral suppression and optimal care [24]. Circulating sCD163, the soluble ectodomain of the macrophage scavenger receptor released in response to inflammatory stimuli, remains elevated in PLWH and has been associated with vascular inflammation, atherosclerotic progression, and

EARLY ACCESS

adverse clinical outcomes, including all-cause and cardiovascular mortality as well as incident heart failure [25].

Previous studies indicate that sCD163 trajectories under ART are context dependent. In the randomized ACTG 5260s trial [26], sCD163 declined similarly among ART-naïve adults initiating atazanavir/ritonavir (ATV/r), darunavir/ritonavir (DRV/r) or RAL with TDF/FTC, consistent with reduced immune activation under effective ART. In contrast, another randomized study that included participants with HBV/HCV coinfection reported increased sCD163 after switching from efavirenz/TDF/FTC to RAL/TDF/FTC over 24 weeks, with no change in VCAM-1 [27]. Together, these differing trajectories suggest that changes in sCD163 may depend on host context, including coinfection and baseline inflammatory status, rather than on ART class alone.

In a retrospective cohort of ART-naïve adults starting INSTI- or ATV-based therapy, 12 months of treatment was associated with biomarker changes from baseline [28]. Among participants receiving unboosted INSTIs, TNF-α decreased only with dolutegravir (DTG), sCD14 decreased with RAL and DTG, and sCD163 decreased with RAL as well as with PI-based regimens. IL-10, an anti-inflammatory cytokine with atheroprotective effects in experimental models [29], increased in our study but not in this retrospective comparator [28], and remains incompletely characterized in ART initiation or switch studies.

Although no lipid feature remained significant after FDR correction, 26 features had large observed absolute paired Hedges' g_z point estimates. Most of these estimates were positive and involved glycerophospholipids, particularly PC and PE features. Given the uncertainty associated with a sample of 11 participants and the absence of FDR-significant results, these patterns do not support biological or mechanistic conclusions. They are reported solely to generate hypotheses for validation in larger, independent cohorts.

This study has several limitations. First, the sample of 11 participants provided limited power and precision, particularly given the multiple-testing burden of untargeted lipidomics. Large observed standardized effects may therefore reflect sampling variability, whereas the absence of FDR-significant findings should not be interpreted as evidence of equivalence or absence of a biologically relevant effect.

EARLY ACCESS

Second, although run-level quality control and feature curation were applied, study-specific within-assay and between-assay CVs were not available for every analyte. Third, the absence of an alternative-regimen comparator prevents separation of regimen-specific effects from changes related to ART initiation, viral suppression, time, or other time-varying factors. The within-participant design reduces inter-individual variability but does not address time-varying confounding. Fourth, fasting status and information on BMI, lipid-lowering therapy, conventional lipid profiles, smoking, alcohol consumption, concomitant medications, socioeconomic factors, and diet were unavailable or inconsistently recorded. Exclusion of participants with diabetes or established CVD reduced, but did not eliminate, potential metabolic confounding. Finally, the eligibility criteria, including a baseline CD4+ T-cell count ≥200 cells/μL and exclusion of hepatitis B or C coinfection, recent AIDS-defining conditions, pregnancy, established CVD, and diabetes, limit generalizability to populations with advanced disease, coinfections, or major cardiometabolic comorbidity.

CONCLUSION

In this small, uncontrolled cohort, IL-10 concentrations were higher and sCD163 concentrations were lower at follow-up than at baseline after correction for multiple testing, whereas no lipid feature remained significant after FDR correction. The lipid effect-size estimates identify exploratory candidates for future study but do not establish a treatment-specific lipidomic signature. These findings are descriptive and hypothesis-generating and cannot be attributed specifically to RAL plus TDF/FTC. Larger controlled studies are needed to assess their reproducibility and regimen specificity.

EARLY ACCESS

ACKNOWLEDGMENTS

The authors gratefully acknowledge the patients for their participation and the indispensable contributions of the medical and nursing personnel, the data managers, and the HIV BioBank integrated in the Spanish AIDS Research Network and collaborating Centers of CoRIS for the generous gifts of clinical samples and patient´s data used in this work (see **group authorship** for a complete list of authors and centers contributing to CoRIS and to HIV Biobank). The HIV BioBank, integrated in

the Spanish AIDS Research Network, is supported by Institute of Health Carlos III, ISCIII, Spanish Health Ministry (Grants n° RD06/0006/0035; RD12/0017/0037 and RD16/0025/0019) as part of the State Plan for Scientific and Technical Research and Innovation and cofinanced by ISCIII–Sub-Directorate General for Research Assessment and Promotion and European Regional Development Fund (ERDF). This study would not have been possible without the collaboration of medical, nursery staff and data managers who have taken part in the project. The RIS Cohort (CoRIS) is funded by the ISCIII through the Spanish AIDS Research Network (RIS C03/173 and RD12/0017/0018) as part of the State Plan for Scientific and Technical Research and Innovation and co-financed by ISCIII–Sub-Directorate General for Research Assessment and Promotion and European Regional Development Fund (ERDF).
The authors acknowledge the use of ChatGPT (OpenAI, GPT-5) solely for language editing and style refinement of the English text. The scientific content, study design, data analysis, and conclusions are entirely the authors' own.

Conflicts of interest: JRB reports consulting and lecture fees from Gilead Sciences, Merck, Moderna, Pfizer and ViiV Healthcare, and grants and payments for the development of educational presentations from Gilead Sciences and ViiV Healthcare. EB reports honoraria for lectures from Gilead, ViiV, and Janssen, and research study grants from Gilead. DR-C reports grants as speaker from ViiV Healthcare and Gilead Science. MMV and CA are employees of Rubio Metabolomics, SLU. LP-M reports compensation for lectures from Gilead Sciences and Janssen. All other authors declare no competing interests.

Funding: This study was supported by Project PI20/00735 (Instituto de Salud Carlos III [ISCIII], Acción Estratégica en Salud, cofinanciado a través del Fondo Europeo de Desarrollo Regional (FEDER). This research was supported by CIBER -Consorcio Centro de Investigación Biomédica en Red-(CB21/13/00091), Instituto de Salud Carlos III, Ministerio de Ciencia e Innovación and Unión Europea – NextGenerationEU. The HIV BioBank is supported by Instituto de Salud Carlos III (PT20/00138) and Networking Research Center on Bioengineering, Biomaterials and Nanomedicine, CIBER-BBN (CB22/01/00041).

Data availability: Due to ethical considerations, access to the study data is restricted. Reasoned requests for data should be submitted to the Spanish AIDS Cohort Research Network and directed to the corresponding authors for evaluation.

EARLY ACCESS

Submitted: August 24, 2026
Accepted: September 28, 2026
Published online: October 19, 2026

EARLY ACCESS

GROUP AUTHORSHIP

Centres and investigators involved in the CoRIS cohort are listed below:

CoRIS Executive committee:

Santiago Moreno, Inma Jarrín, David Dalmau, M Luisa Navarro, Federico Garcia, Eva Poveda, Jose Antonio Iribarren, Félix Gutiérrez, Francesc Vidal, Juan Berenguer, Juan González.

Centres and investigators involved in CoRIS cohort are listed below:

CoRIS Coordination Unit

Inma Jarrín, Cristina Moreno, Marta Rava, Rebeca Izquierdo, Cristina Marco-Sánchez, Teresa Gómez-García.

BioBanK HIV Hospital General Universitario Gregorio Marañón

José Luis Jiménez.

Hospital General Universitario Dr Balmis (Alicante)

Sergio Reus, Irene Portilla, Esperanza Merino, Gema García, José Sánchez-Payá, Juan Carlos Rodríguez, Livia Giner, Joaquín Portilla, Vicente Boix, Diego Torrus, Julia Portilla-Tamarit, Héctor Pinargote.

Hospital Universitario de Canarias (San Cristóbal de la Laguna)

María Remedios Alemán, Nereyda Tosco-García, Ana López Lirola, Dácil García, Felicitas Díaz-Flores, María del Mar Alonso, Ricardo Pelazas, María Inmaculada Hernández, Lucia Romero-Acevedo, Abraham Bethencourt-Padilla, Daniel Rodríguez-Díaz, Ana María Godoy-Reyes.

Hospital Universitario Central de Asturias (Oviedo)

Víctor Asensi, Rebeca Cabo Magadan, Lorena Fernández, Javier Díaz-Arias

Hospital Universitario 12 de Octubre (Madrid)

Federico Pulido, Rafael Rubio, M Asunción Hernando, Otilia Bisbal, David Rial-Crestelo, María de Lagarde, Laura Bermejo, Mireia Santacreu, Juan Martín Torres, Belén Sánchez-López.

EARLY ACCESS

Servicio de Enfermedades Infecciosas. Hospital Universitario Donostia. Instituto de Investigación Sanitaria BioGipuzkoa (Donostia-San Sebastián)

José Antonio Iribarren, Xabier Kortajarena, Claudia Nevado Pavón, Xabier Camino, Miguel Ángel Goenaga, M Jesús Bustinduy, Harkaitz Azkune, Maialen Ibarguren, Ignacio Álvarez-Rodriguez, Leire Gil-Alonso, Francisco Carmona-Torre, Ana Bayona Carlos, Maialen Lekuona Sanz, Leire Balerdi Sarasola, Ander Goyache Moreno.

Hospital General Universitario De Elche (Elche)

Félix Gutiérrez, Catalina Robledano, Mar Masiá, Sergio Padilla, Rafael Pascual, Marta Fernández, Antonio Galiana, José Alberto García, Xavier Barber, Javier García Abellán, Guillermo Telenti, Ángela Botella, Paula Mascarell, Lidia García-Sánchez, Nuria Ena, Leandro López, Jennifer Vallejo, Nieves Gonzalo-Jiménez, Montserrat Ruiz, Christian Ledesma, Santiago López, María Espinosa-Pérez, Ana Quiles, María del Mar Alcalde-Encinas, José García-García, Rosario Hernández-Ros, José Carlos Escribano, Marouane Menchi-Elanci, María del Mar García Navarro.

Hospital General Universitario Gregorio Marañón (Madrid)

Cristina Diez, Isabel Gutiérrez, Juan Berenguer, Margarita Ramírez, Teresa Aldamiz-Echevarría, Francisco Tejerina, Leire Pérez-Latorre, Chiara Fanciulli, Saray Corral.

Hospital Universitari de Tarragona Joan XXIII (Tarragona)

Joaquim Peraire, Anna Rull, Anna Martí, Consuelo Viladés, Beatriz Villar, Lluïsa Guillem, Silvia Chafino, Marina Flores, Francesc Vidal.

Hospital Universitario y Politécnico de La Fe (Valencia)

Marta Montero-Alonso, María Tasias-Pitarch, Eva Calabuig-Muñoz, Miguel Salavert-Lletí, Juan Fernández-Navarro, Rosa Blanes-Hernández, Jennifer Sánchez-Guevara.

Hospital Universitario La Paz/IdiPAZ (Madrid)

Juan González-García, José Ignacio Bernardino, Ana Delgado-Hierro, José Ramón Arribas, Víctor Arribas, Juan Miguel Castro, Luis Escosa, Iker Falces, Pedro Herranz-Pinto, Alicia González-Baeza, María Luz Martín-Carbonero, Rafael Micán, Rocío Montejano, María Luisa Montes, Luis Ramos-Ruperto, Berta Rodés Soldevila, Talia Sainz, Elena Sendagorta, Carmen Busca, Joanna Cano-Smith, Rosa de Miguel, María

EARLY ACCESS

del Mar Arcos-Rueda, Alejandro de Gea-Grela, Nerea Iniesta-Arandia, Alejandro Díez-Vidal, María Jesús Roldán-Cabrales, Carlos Oñoro-López, Jara Llenas García, Laura Lucía Checa Daimiel.

Hospital Universitari Mutua Terrassa (Terrassa)

David Dalmau, Marina Martinez, Angels Jaén, Mireia Cairó, Javier Martinez-Lacasa, Roser Font, Laura Gisbert.

Hospital Universitario de La Princesa (Madrid)

Ignacio de los Santos, Alejandro de los Santos, Lucio García-Fraile, Enrique Martín-Gayo, Ildefonso Sánchez-Cerrillo, Ángela Gutiérrez, Carmen Sáez, Ana Barrios Blandino, Azucena Bautista, Marianela Ciudad, María Aguilera García, Violeta Sampériz Rubio, Javier Pérez Serrano, Isabel Belmonte Martín de Santa Olalla.

Hospital Universitario Ramón y Cajal (Madrid)

Santiago Moreno, Santos del Campo, José Luis Casado, Fernando Dronda, Ana Moreno, María Jesús Pérez-Elías, Sergio Serrano-Villar, María Jesús Vivancos-Gallego, Javier Martínez-Sanz, Alejandro Vallejo Tiller, Matilde Sánchez-Conde, José Antonio Pérez-Molina, José Manuel Hermida, Erick De La Torre Tarazona, Elena Moreno del Olmo, Laura Martín Pedraza, Claudio Díaz García, Jorge Díaz Álvarez, Alejandro García-García, Raquel Ron-González, Sergio Calderón Vicente, Roser Navarro Soler, Sara Saiz-Baggetto, Ana del Amo-de Palacios, Laura Luna, Miguel Antón Ámez Segovia, Sara Martín Colmenarejo, Cristina Chica.

Hospital General Universitario Reina Sofía (Murcia)

Enrique Bernal, María Dolores Hernández, Antonia Alcaraz, Joaquín Bravo, Ángeles Muñoz Pérez, Cristina Tomás Jimenez, Salvador Valero Cifuentes, Eva García-Villalba, Román González Hipólito, Elena Guijarro-Westermeyer, Rodrigo Martínez-Rodríguez, José Miguel Gómez Verdú.

Hospital Universitario Clínico San Cecilio (Granada)

Federico García, Clara Martínez, Maite Laperal, Leopoldo Muñoz Medina, Marta Álvarez-Estevez, Natalia Chueca-Porcuna, David Vinuesa-García, Adolfo de Salazar-González, Ana Fuentes-López, Emilio Guirao, Andrés Ruiz-Sancho, Francisco Anguita, Naya Faro, Lucia Chaves, Marta Illescas, Paloma Muñoz-Baez, Lucía Pérez,

EARLY ACCESS

Ana Alberola Romano, Alberto Vazquez Blanquiño, Lucía Guillén-Zafra, Javier Martínez de Victoria-Carazo.

Centro Sanitario Sandoval (Madrid)

Jorge Del Romero-Guerrero, Montserrat Raposo, Teresa Puerta-López, Mar Vera, Juan Ballesteros, Begoña Baza, Laura Dans Villán, Ruben Linares Navarro, Ines Armenteros Yeguas, Eva Orviz-García, Santiago Fernández Castelao.

Hospital Universitario Son Espases (Palma de Mallorca)

Melchor Riera, Antonio Vanrell, María Peñaranda, Mª Angels Ribas, Antoni A. Campins, Mercedes Garcia-Gasalla, Francisco J Fanjul, Javier Murillas-Angoiti, Luisa Martin-Pena, Francisca Artigues, Sophia Pinecki, Adrián Ferre.

Hospital Universitario Virgen de la Victoria (Málaga)

Jesús Santos, María López-Jódar, Cristina Gómez-Ayerbe, Isabel Viciana, Rosario Palacios.

Hospital Universitario Virgen del Rocío (Sevilla)

Luis Fernando López-Cortés, Silvia Llaves-Flores, Inmaculada Rivas Jeremías, Nuria Espinosa, Cristina Roca-Oporto, Marta Herreros-Romero, César Sotomayor de la Piedra, Abraham Saborido Alconchel, Manuel Francisco Liroa, Jesús Fernández Plaza.

Hospital Universitario de Bellvitge (Hospitalet de Llobregat)

Juan Manuel Tiraboschi, Arkaitz Imaz, María Saumoy, Analuz Fernandez, Jaime Vega Costa, Daniel Medina Gamito.

Hospital Costa del Sol (Marbella)

Julián Olalla, Javier Pérez, Alfonso del Arco, Javier de la Torre, Francisca Ruiz.

Hospital General Universitario Santa Lucía (Cartagena)

Onofre Juan Martínez, Lorena Martinez, Francisco Jesús Vera, Josefina García, Begoña Alcaraz, Sergio Guillén Martínez, Patricia Carles García.

Complejo Hospitalario Universitario a Coruña (CHUAC) (A Coruña)

Álvaro Mena, Berta Pernas, Pilar Vázquez, Soledad López, Brais Castelo.

Hospital Universitario Virgen de la Arrixaca (El Palmar)

EARLY ACCESS

Carlos Galera, Marian Fernández, Helena Albendin, Antonia Castillo, Asunción Iborra, Antonio Moreno, M Angustias Merlos, Almudena Ortuño.

Hospital Universitario Infanta Sofía (San Sebastián de los Reyes)

Inés Suarez-García, Eduardo Malmierca, Patricia González-Ruano, M Pilar Ruiz, Luz Balsalobre, Ángela Somodevilla, Rebeca Fuerte Martínez.

Hospital Clínico San Carlos (Madrid)

Vicente Estrada, Nieves Sanz, Noemí Cabello-Clotet, María José Núñez, Ana Muñoz, Juncal Pérez-Somarriba, Reynaldo Homen, Rafael Rubio-Martín, Susana Olmedo, Julia Barrado.

Hospital Universitario Príncipe de Asturias (Alcalá de Henares)

José Sanz, Cristina Hernández-Gutiérrez, María Novella-Mena.

Hospital Clínico Universitario de Valencia (Valencia)

María José Galindo, Sandra Pérez Gómez, Ana Ferrer, Anaís Corma Gómez.

Hospital Reina Sofía (Córdoba)

Antonio Rivero-Román, Laura Ruiz-Torres, Antonio Rivero-Juárez, Pedro López-López, Mario Frias-Casas, Ángela Camacho, Ignacio Pérez, Diana Corona, Javier Manuel Caballero, Marina Gallo Marín, María Casares, Lucía Ríos-Muñoz, Claudia Ferreira-Tata, María Carrasquilla.

Hospital Universitario Severo Ochoa (Leganés)

Rafael Rodríguez-Rosado Martinez-Echevarría.

Hospital Universitario Virgen de Valme (Sevilla)

Juan Macías Sánchez, Pilar Rincón, Luis Miguel Real, Jésica Martín-Carmona.

Hospital Álvaro Cunqueiro (Vigo)

Eva Poveda, Alexandre Pérez, Luis Morano, Celia Miralles, Antonio Ocampo, Jacobo Alonso, Inés Martínez, Aida López-López.

Hospital Universitario Marqués de Valdecilla (Santander)

EARLY ACCESS

M Carmen Fariñas Álvarez, Claudia González Rico, Noelia Ruiz Alonso, Carlos Armiñanzas Castillo, Francisco Arnaiz de las Revillas Almajano, Manuel Gutiérrez Cuadra, Raúl Parra Fariñas, Paula Runza Buznego, Aitziber Illaro Uranga.

Hospital Clínic de Barcelona (Barcelona)

José Luis Blanco Arévalo, Pilar Callau Cabrera, Josep Mallolas Masferrer, José Alcamí Pertejo, Sonsoles Sánchez-Palomino, Núria Climent, Ana González-Cordón, Montse Laguno Centeno, María Martínez-Rebollar, Juan Ambrosioni, Berta Torres, Lorena de la Mora, Alexy Inciarte, Esteban Martínez, José María Miró, Abiu Sempere, Julia Calvo, Iván Chivite, David García, Alberto Foncillas, Daniela Malano, Montse Plana, Roger Llobet, Estela Solbes, Octavi Roman, Rona Sagarra, Vanesa Guilera, Gemma Olmeda, Paula Arreba, María José Rodríguez, Emma Fernández, Ana Rodríguez, Alba ortega, Sergi Anguera, Raquel Aguiló, Laura Novell.

Centro Nacional de Microbiología (Majadahonda)

Luis Miguel Bedoya Del Olmo, Manuela Beltran Vicente, Mercedes Bermejo Herrero, Maria Esther Calonge Errejon, Laura Capa Muñoz, Maria Teresa Coiras Lopez, Francisco Diez Fuertes, Javier Garcia Perez, Nuria Gonzalez Fernandez, Elena Mateos De Las Moreras, Maria Teresa Perez Olmeda, Victor Sanchez Merino, Maria Eloisa Yuste Herranz.

Centro Nacional de Biotecnología. Consejo Superior de Investigaciones Científicas (CSIC) (Madrid)

Carmen Elena Gomez Rodriguez, Juan Francisco Garcia Arriaza, Laura Sin Diaz, Beatriz Perdiguero de la Torre, Laura Marcos Villar, Patricia Perez Ramirez, Enrique Alvarez Coruña, David Astorgano Lopez, Cristina Sanchez Corzo.

EARLY ACCESS

REFERENCES

1. Angelidou K, Hunt PW, Landay AL, Wilson CC, Rodriguez B, Deeks SG, et al. Changes in inflammation but not in T-cell activation precede non-AIDS-defining events in a case-control study of patients on long-term antiretroviral therapy. J Infect Dis. 2018;218(2):239–48. https://doi.org/10.1093/infdis/jix666
2. Clotet B, Feinberg J, van Lunzen J, Khuong-Josses MA, Antinori A, Dumitru I, et al. Once-daily dolutegravir versus darunavir plus ritonavir in antiretroviral-naive adults with HIV-1 infection (FLAMINGO): 48 week results from the randomised open-label phase 3b study. Lancet. 2014;383(9936):2222–31. https://doi.org/10.1016/S0140-6736(14)60084-2
3. Brennan AT, Nattey C, Kileel EM, Rosen S, Maskew M, Stokes AC, et al. Change in body weight and risk of hypertension after switching from efavirenz to dolutegravir in adults living with HIV: evidence from routine care in Johannesburg, South Africa. EClinicalMedicine. 2023;57:101836. https://doi.org/10.1016/j.eclinm.2023.101836
4. O'Halloran JA, Sahrmann J, Parra-Rodriguez L, Vo DT, Butler AM, Olsen MA, et al. Integrase strand transfer inhibitors are associated with incident diabetes mellitus in people with human immunodeficiency virus. Clin Infect Dis. 2022;75(12):2060–5. https://doi.org/10.1093/cid/ciac355
5. Chai JC, Deik AA, Hua S, Wang T, Hanna DB, Xue X, et al. Association of lipidomic profiles with progression of carotid artery atherosclerosis in HIV infection. JAMA Cardiol. 2019;4(12):1239–49. https://doi.org/10.1001/jamacardio.2019.4025
6. Sacks FM, Lichtenstein AH, Wu JHY, Appel LJ, Creager MA, Kris-Etherton PM, et al. Dietary fats and cardiovascular disease: a presidential advisory from the American Heart Association. Circulation. 2017;136(3):e1–e23. https://doi.org/10.1161/CIR.0000000000000510
7. Yamada H, Yoshida M, Nakano Y, Suganami T, Satoh N, Mita T, et al. In vivo and in vitro inhibition of monocyte adhesion to endothelial cells and endothelial adhesion molecules by eicosapentaenoic acid. Arterioscler Thromb Vasc Biol. 2008;28(12):2173–9. https://doi.org/10.1161/ATVBAHA.108.171736

EARLY ACCESS

8. Trevillyan JM, Wong G, Puls R, Petoumenos K, Emery S, Mellett NA, et al. Changes in plasma lipidome following initiation of antiretroviral therapy. PLoS One. 2018;13(8):e0202944. https://doi.org/10.1371/journal.pone.0202944
9. Ghosh A, Nishtala K. Biofluid lipidome: a source for potential diagnostic biomarkers. Clin Transl Med. 2017;6(1):22. https://doi.org/10.1186/s40169-017-0152-7
10. Wenk MR. The emerging field of lipidomics. Nat Rev Drug Discov. 2005;4(7):594–610. https://doi.org/10.1038/nrd1776
11. Sivanandham S, Sivanandham R, Xu C, Symmonds J, Sette P, He T, et al. Plasma lipidomic alterations during pathogenic SIV infection with and without antiretroviral therapy. Front Immunol. 2025;16:1475160. https://doi.org/10.3389/fimmu.2025.1475160
12. Jao J, Balmert LC, Sun S, McComsey GA, Brown TT, Tien PC, et al. Distinct lipidomic signatures in people living with HIV: combined analysis of ACTG 5260s and MACS/WIHS. J Clin Endocrinol Metab. 2022;107(1):119–35. https://doi.org/10.1210/clinem/dgab663
13. Chaudhary NS, Kind T, Willig AL, Saag MS, Shrestha S, Funderburg N, et al. Changes in lipidomic profile by anti-retroviral treatment regimen: an ACTG 5257 ancillary study. Medicine (Baltimore). 2021;100(30):e26588. https://doi.org/10.1097/MD.0000000000026588
14. Scarsi KK, Havens JP, Podany AT, Avedissian SN, Fletcher CV. HIV-1 integrase inhibitors: a comparative review of efficacy and safety. Drugs. 2020;80(16):1649–76. https://doi.org/10.1007/s40265-020-01379-9
15. Dow DE, Bartlett JA. Dolutegravir, the second-generation of integrase strand transfer inhibitors (INSTIs) for the treatment of HIV. Infect Dis Ther. 2014;3(2):83–102. https://doi.org/10.1007/s40121-014-0029-7
16. Caro-Murillo AM, Castilla J, Perez-Hoyos S, Miro JM, Podzamczer D, Rubio R, et al. [Spanish cohort of naive HIV-infected patients (CoRIS): rationale, organization and initial results]. Enferm Infecc Microbiol Clin. 2007;25(1):23–31. https://doi.org/10.1157/13096749
17. Sobrino-Vegas P, Gutierrez F, Berenguer J, Labarga P, Garcia F, Alejos-Ferreras B, et al. [The cohort of the Spanish HIV Research Network (CoRIS) and its associated biobank; organizational issues, main findings and losses to follow-up].

EARLY ACCESS

Enferm Infecc Microbiol Clin. 2011;29(9):645–53. https://doi.org/10.1016/j.eimc.2011.06.002

18. Garcia-Merino I, de Las Cuevas N, Jimenez JL, Gallego J, Gomez C, Prieto C, et al. The Spanish HIV BioBank: a model of cooperative HIV research. Retrovirology. 2009;6:27. https://doi.org/10.1186/1742-4690-6-27
19. Barr J, Caballeria J, Martinez-Arranz I, Dominguez-Diez A, Alonso C, Muntane J, et al. Obesity-dependent metabolic signatures associated with nonalcoholic fatty liver disease progression. J Proteome Res. 2012;11(4):2521–32. https://doi.org/10.1021/pr201223p
20. Liebisch G, Fahy E, Aoki J, Dennis EA, Durand T, Ejsing CS, et al. Update on LIPID MAPS classification, nomenclature, and shorthand notation for MS-derived lipid structures. J Lipid Res. 2020;61(12):1539–55. https://doi.org/10.1194/jlr.S120001025
21. Martinez-Arranz I, Mayo R, Perez-Cormenzana M, Minchole I, Salazar L, Alonso C, et al. Enhancing metabolomics research through data mining. J Proteomics. 2015;127(Pt B):275–88. https://doi.org/10.1016/j.jprot.2015.01.019
22. Lakens D. Calculating and reporting effect sizes to facilitate cumulative science: a practical primer for t-tests and ANOVAs. Front Psychol. 2013;4:863. https://doi.org/10.3389/fpsyg.2013.00863
23. Bowman ER, Kulkarni M, Gabriel J, Cichon MJ, Riedl K, Belury MA, et al. Altered lipidome composition is related to markers of monocyte and immune activation in antiretroviral therapy treated human immunodeficiency virus (HIV) infection and in uninfected persons. Front Immunol. 2019;10:785. https://doi.org/10.3389/fimmu.2019.00785
24. Obare LM, Stephens VR, Wanjalla CN. Understanding residual risk of cardiovascular disease in people with HIV. Curr Opin HIV AIDS. 2025;20(4):319–30. https://doi.org/10.1097/COH.0000000000000953
25. Durda P, Raffield LM, Lange EM, Olson NC, Jenny NS, Cushman M, et al. Circulating soluble CD163, associations with cardiovascular outcomes and mortality, and identification of genetic variants in older individuals: the Cardiovascular Health Study. J Am Heart Assoc. 2022;11(21):e024374. https://doi.org/10.1161/JAHA.121.024374
26. Kelesidis T, Tran TT, Stein JH, Brown TT, Moser C, Ribaudo HJ, et al. Changes in inflammation and immune activation with atazanavir-, raltegravir-, darunavir-

EARLY ACCESS

based initial antiviral therapy: ACTG 5260s. Clin Infect Dis. 2015;61(4):651–60. https://doi.org/10.1093/cid/civ327

27. Gupta SK, Mi D, Moe SM, Dube MP, Liu Z. Effects of switching from efavirenz to raltegravir on endothelial function, bone mineral metabolism, inflammation, and renal function: a randomized, controlled trial. J Acquir Immune Defic Syndr. 2013;64(3):279–83. https://doi.org/10.1097/QAI.0b013e3182a97c39
28. Quiros-Roldan E, Castelli F, Bonito A, Vezzoli M, Calza S, Biasiotto G, et al. The impact of integrase inhibitor-based regimens on markers of inflammation among HIV naive patients. Cytokine. 2020;126:154884. https://doi.org/10.1016/j.cyto.2019.154884
29. Perez Fernandez R, Kaski JC. [Interleukin-10 and coronary disease]. Rev Esp Cardiol. 2002;55(7):738–50. https://doi.org/10.1016/S0300-8932(02)76693-1

EARLY ACCESS

TABLES AND FIGURES WITH LEGENDS

Table 1. Longitudinal changes in circulating biomarkers from baseline to week 48

Variable	Baseline, median (Q1-Q3)	Follow-up, median (Q1-Q3)	Hodges-Lehmann change (95% CI)	*p* (paired Wilcoxon)	*q* (BH-FDR)	Paired Hedges' g_z (95% CI)
Pro- and anti-inflammatory biomarkers						
CRP (ng/ml)	1486.096 (1000.263-1724.779)	1383.874 (1064.085–1624.501)	-97.083 (-376.528, 222.500)	0.577	0.783	-0.154 (-1.099, 0.395)
TNF (fg/ml)	46.053 (37.785–51.150)	45.618 (44.097–51.370)	1.905 (-3.495, 7.068)	0.577	0.783	0.156 (-0.400, 1,001)
IL-6 (fg/ml)	42.152 (37.888–45.585)	47.718 (41.689–51.802)	4.363 (-2.771, 10.004)	0.175	0.369	0.416 (-0.117, 1.449)
IL-8 (fg/ml)	28.374 (23.216–32.741)	33.498 (23.901–49.216)	6.902 (-0.180, 15.015)	0.054	0.201	0.631 (0.207, 1.269)
IL-10 (fg/ml)	14.613 (11.292–17.563)	34.434 (28.778–38.859)	20.675 (15.268, 43.726)	**<0.001**	**0.019**	1.209 (0.993, 4.747)
Immune activation biomarkers						
CD40 (ng/ml)	5.260 (3.170–6.819)	6.064 (3.902–7.794)	0.556 (-1.316, 2.049)	0.413	0.654	0.121 (-0.303, 0.967)
sCD163 (ng/ml)	957.734 (591.254–1244.760)	470.019 (422.181–691.762)	-357.966 (-818.026, -173.161)	**0.002**	**0.019**	-0.878 (-2.343, -0.631)
sCD14 (ng/ml)	2.866 (2.174–3.388)	2.707 (2.046–3.006)	-0.059 (-0.849, 0.687)	0.966	0.966	-0.068 (-0.717, 0.582)
LBP (ng/ml)	18.155 (14.908–21.566)	16.456 (14.692–21.958)	0.563 (-4.359, 3.116)	0.765	0.908	-0.045 (-0.610, 0.668)
Endothelial and vascular dysfunction markers						
ICAM-1(ng/ml)	74.640 (61.231–82.012)	62.982 (52.680–73.516)	-11.215 (-23.337, 1.694)	0.074	0.201	-0.589 (-1.175, -0.140)
VCAM-1 (ng/ml)	805.144 (675.209–1028.166)	669.415 (536.491–689.618)	-173.727 (-2158.811, -12.087)	**0.032**	0.201	-0.465 (-0.846, -0.300)
E-selectin (ng/ml)	30.593 (22.862–40.993)	32.855 (25.569–50.245)	4.199 (-5.774, 17.146)	0.413	0.654	0.309 (-0.294, 0.850)
P-selectin (ng/ml)	31.024 (28.442–32.942)	40.622 (31.535–42.029)	6.354 (-0.588, 11.523)	0.054	0.201	0.687 (0.117, 2.088)
sP-selectin (ng/ml)	46.060 (39.418–78.031)	56.279 (44.746–65.695)	3.504 (-21.460, 25.036)	0.638	0.808	0.082 (-0.570, 0.617)

Adipokine markers						
Leptin (ng/ml)	0.034 (0.029–0.175)	0.041 (0.035–0.220)	0.010 (-0.003, 0.078)	0.064	0.201	0.377 (-0.061, 1.223)
Adiponectin (ng/ml)	10.431 (7.858–12.083)	9.680 (7.870–13.936)	-1.241 (-3.386, 4.506)	0.320	0.609	0.012 (-1.311, 0.472)
Tryptophan metabolism						
Tryptophan (ng/ml)	2.357 (1.662–2.743)	2.062 (1.551–2.208)	-0.285 (-0.743, 0.171)	0.175	0.369	-0.432 (-1.372, 0.105)
Kynurenic acid (ng/ml)	23.390 (19.815–28.181)	23.186 (22.553–24.471)	-0.076 (-4.142, 3.658)	0.966	0.966	-0.045 (-0.655, 0.614)
Quinolinic acid (ng/ml)	7.687 (6.441–8.661)	7.240 (6.511–8.563)	-0.041 (-0.925, 0.665)	0.831	0.929	-0.077 (-0.652, 0.582)

Values are medians (Q1-Q3). Follow-up was defined as the assessment closest to 48 weeks after ART initiation for each participant (range, 47.7-61.9 weeks). Change is the Hodges-Lehmann pseudomedian of the paired differences (follow-up - baseline) with a 95% CI. *p* values were obtained using paired Wilcoxon signed-rank tests, with the exact procedure used where possible. Zero paired differences do not contribute to the signed-rank statistic but are included in the reported paired sample size. q values were obtained using the Benjamini-Hochberg false discovery rate procedure across the direct biomarker family. Paired Hedges' g_z is reported with a bootstrap 95% CI. **Abbreviations**: ART, antiretroviral therapy; BH-FDR, Benjamini–Hochberg false discovery rate; CD40, cluster of differentiation 40; CI, confidence interval; CRP, C-reactive protein; E-selectin, endothelial selectin; ICAM-1, intercellular adhesion molecule-1; IL-10, interleukin-10; IL-6, interleukin-6; IL-8, interleukin-8; LBP, lipopolysaccharide-binding protein; P-selectin, platelet selectin; Q1, first quartile; Q3, third quartile; sCD14, soluble cluster of differentiation 14; sCD163, soluble cluster of differentiation 163; sP-selectin, soluble platelet selectin; TNF, tumor necrosis factor; VCAM-1, vascular cell adhesion molecule-1.

EARLY ACCESS

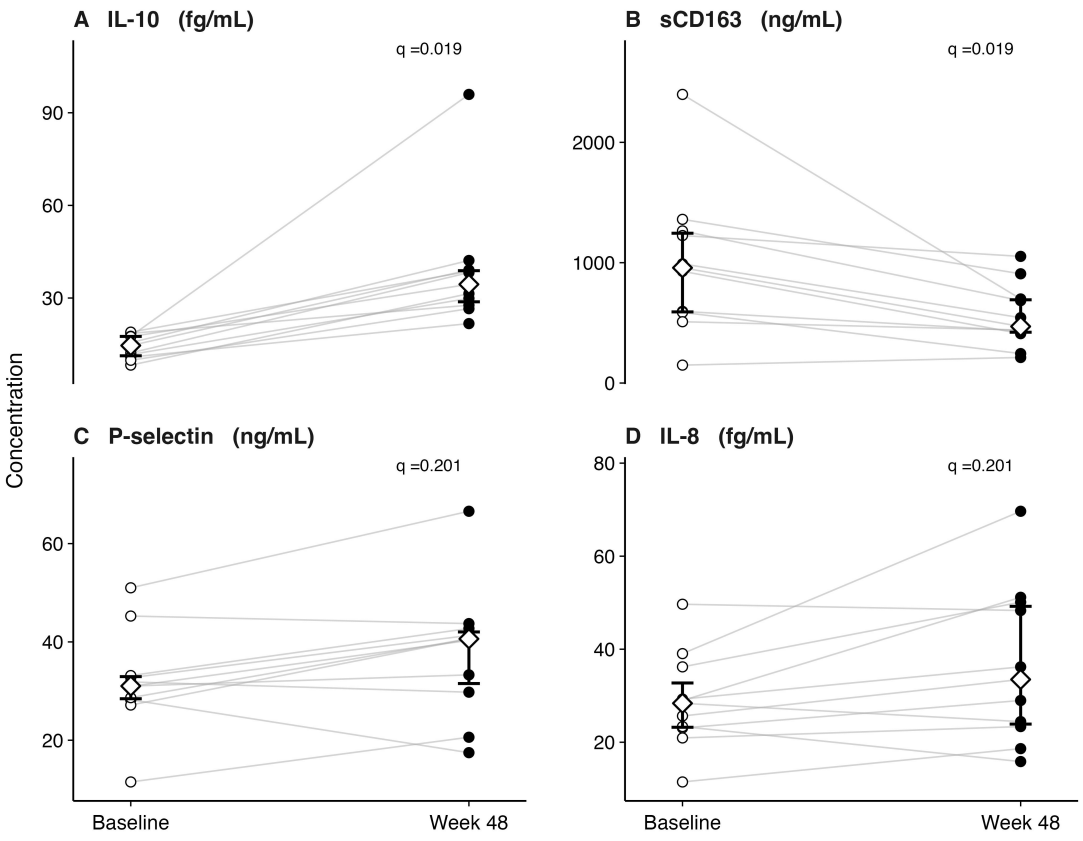


Figure 1. Paired longitudinal changes in circulating biomarkers following ART initiation. Concentrations of **(A)** IL-10, **(B)** sCD163, **(C)** P-selectin, and **(D)** IL-8 are shown at baseline and follow-up in 11 ART-naïve adults with HIV initiating raltegravir plus tenofovir disoproxil fumarate/emtricitabine. Open circles represent baseline measurements, filled black circles represent follow-up measurements, and gray lines connect measurements from the same participant. Open diamonds indicate medians, and black vertical bars represent interquartile ranges. Follow-up, labeled "Week 48," denotes the available sample collected closest to 48 weeks after ART initiation (range, 47.7–61.9 weeks). Within-participant changes were assessed using two-sided paired Wilcoxon signed-rank tests, with BH-FDR correction applied across the full circulating biomarker panel. Adjusted q values are displayed in each panel, with $q < 0.05$ considered statistically significant. **Abbreviations**: ART, antiretroviral therapy; BH-FDR, Benjamini–Hochberg false discovery rate; HIV, human immunodeficiency virus; IL-10, interleukin-10; IL-8, interleukin-8; P-selectin, platelet selectin; sCD163, soluble cluster of differentiation 163.

SUPPLEMENTAL DATA

Table S1. Paired longitudinal analysis of all lipidomic features from baseline to week 48.

Table S2. Lipid features with large observed absolute effect-size estimates (Hedges' $gz \geq 0.80$).

Note: Follow-up denotes the sample collected closest to 48 weeks after ART initiation for each participant (range, 47.7–61.9 weeks).

Table S3. Lipid metabolites, grouped by metabolic class and ranked by effect size (Hedges' g, highest to lowest).

Tables S1–S3 are provided in the accompanying Excel file.

EARLY ACCESS

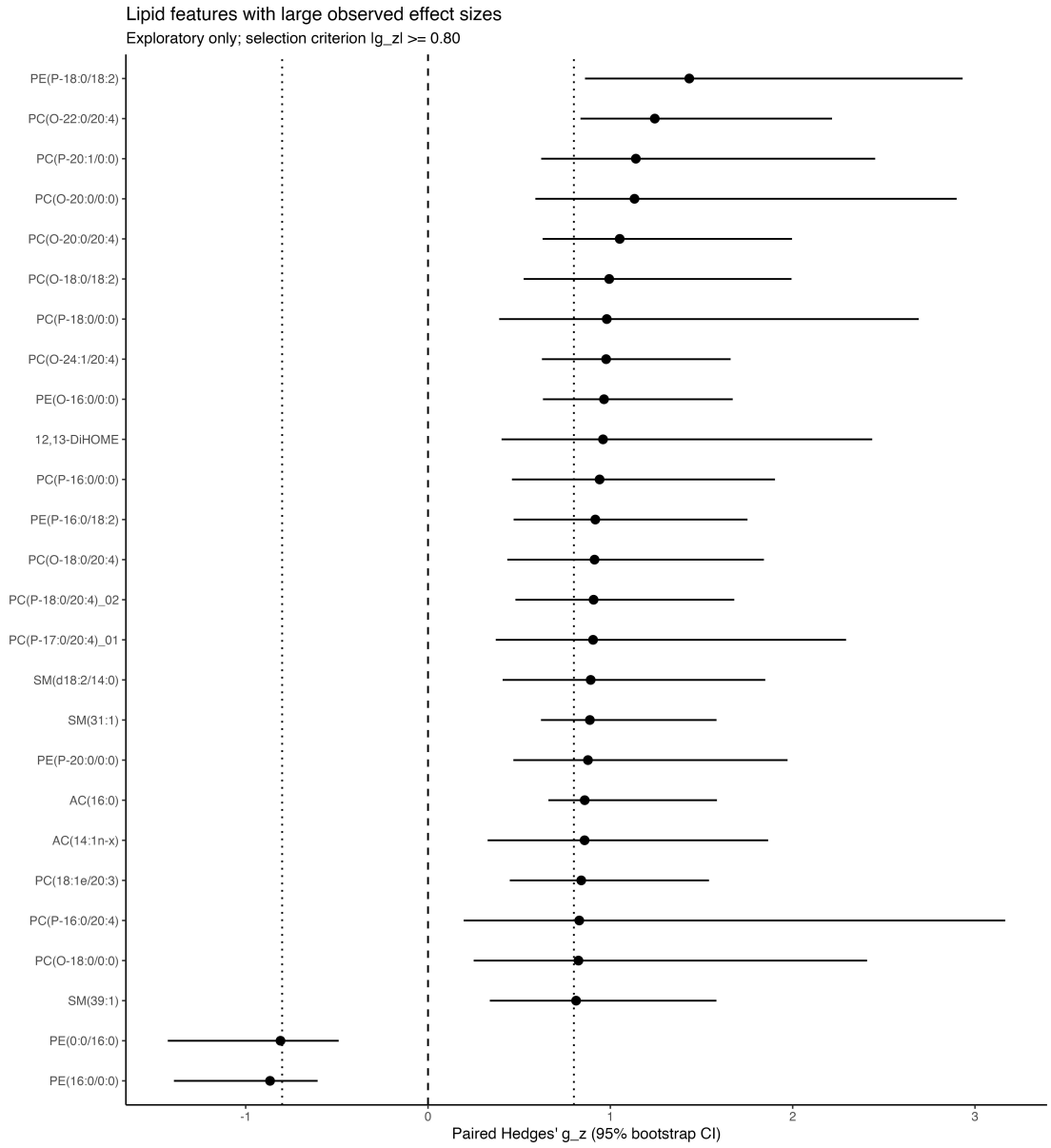


Figure S1. Exploratory paired effect-size estimates for selected lipid features. The forest plot shows 26 of 490 analyzed lipid features with large observed absolute paired Hedges' (g_z) estimates (($|g_z|$ \geq 0.80)) in 11 participants following ART initiation. Features are ordered by decreasing signed effect-size estimate. Points represent paired Hedges' (g_z) estimates, and horizontal lines indicate 95% CIs obtained from 10,000 bootstrap resamples. Positive and negative estimates indicate increases and decreases from baseline to follow-up, respectively. Follow-up corresponds to the available sample collected closest to 48 weeks after ART initiation (range, 47.7–61.9 weeks). The dashed vertical line marks zero, and dotted vertical lines mark the descriptive effect-size thresholds of −0.80 and 0.80. The CIs are not adjusted for multiple testing. Selection was based on observed effect-size magnitude

and does not establish statistical significance; none of the 490 lipid features remained significant after BH-FDR correction. These findings are hypothesis-generating. **Abbreviations**: 12,13-DiHOME, 12,13-dihydroxy-9-octadecenoic acid; AC, acylcarnitine; ART, antiretroviral therapy; BH-FDR, Benjamini–Hochberg false discovery rate; CI, confidence interval; PC, phosphatidylcholine; PE, phosphatidylethanolamine; SM, sphingomyelin.

EARLY ACCESS